Experimental Thermal and Fluid Science 35 (2011) 1497–1504

Contents lists available at ScienceDirect

Experimental Thermal and Fluid Science

journal homepage: www.elsevier.com/locate/etfs

Sail aerodynamics: Understanding pressure distributions on upwind sails

Ignazio Maria Viola [a,b,*], Richard G.J. Flay [a]

[a] Yacht Research Unit, The University of Auckland, New Zealand[1]
[b] School of Marine Science and Technology, Newcastle University, UK[2]

ARTICLE INFO

Article history:
Received 29 January 2011
Received in revised form 24 June 2011
Accepted 26 June 2011
Available online 20 July 2011

Keywords:
Sail aerodynamics
Upwind sails
Mainsails
Headsails
Pressure distributions
Wind tunnel tests

ABSTRACT

The pressure distributions on upwind sails is discussed and related to the flow field around the headsail and the mast/mainsail. Pressures measured on several horizontal sections of model-scale and full-scale sails are used to provide examples. On the leeward side of the sails, leading edge separation and turbulent reattachment occurs, sometimes followed by trailing edge separation. On the windward side, leading edge separation occurs on the mast/mainsail and, at low angles of attack, it can also occur on the headsail. Differences were found between the leading edge bubbles on the two sails. Pressure trends for different angles of attack are presented, and these can be explained in terms of standard aerodynamic theory, particularly in terms of short and long leading edge separation bubble types. It was found that the pressure distributions measured on mainsails at full- and model-scale showed good agreement on both the windward and leeward sides.

1. Introduction

Numerical fluid dynamic methods are widely used to investigate sail aerodynamics. Potential flow codes are normally used to investigate sail aerodynamics in upwind conditions, when a mainsail and a headsail are used and the flow is mainly attached. Conversely, Reynolds Averaged Navier–Stokes techniques, and more recently Large Eddy Simulations, are used to investigate sail aerodynamics in downwind conditions, where the effect of trailing edge separation is not negligible. Although numerical simulations are very effective in investigating sail aerodynamics, they always need to be carefully validated with physical experiments.

Experimental measurements on sails are typically performed in wind tunnels. It is common practice to use flexible sails, which allow the sails to be trimmed. Aerodynamic forces are typically measured with a balance attached to the model. However, pressure measurements allow a more reliable validation of numerical simulations than force measurements. In fact, different pressure distributions can provide the same global aerodynamic forces. However, pressures are rarely measured. In fact, model-scale sails must be light and thin, which makes it difficult for pressure taps to be used. As far as is known to the present authors, pressure distributions on model-scale three-dimensional headsails and mainsails in upwind sailing conditions have never been published. Conversely, pressure distributions on full-scale sails were measured the first time between 1915 and 1921 [10] and much later by the present authors [9], and also by others, e.g. [8,6].

In the present paper, pressure distributions on upwind sails were measured in a wind tunnel on horizontal sections of rigid pressure-tapped sails. Aerodynamic forces were measured with a 6-component balance placed below the model under the wind tunnel floor. The general pressure distributions on the headsail and the mainsail and the correlated flow fields are discussed. The pressure distributions are also compared with the recent full-scale tests performed by the present authors [9].

2. Method

The Yacht Research Unit (YRU) of the University of Auckland has developed an innovative pressure system capable of acquiring up to 512 channels at speeds up to 3900 Hz on each channel. The transducers have a pressure range of ±450 Pa and a resolution of 9.25 mV/Pa. Although initially developed for laboratory use, it has been modified for use on the water. Additional details of the pressure system are provided in Viola and Flay [9]. The system was used to measure the pressures on model-scale rigid pressure-tapped sails, which were designed for the America's Cup class 'AC33'. A 1/15th-scale mainsail and headsail were built as fiberglass sandwich structures. The core was made of a 2 mm thick polypropylene plastic sheet, which had 3 mm wide core

* Corresponding author at: School of Marine Science and Technology, Newcastle University, UK. Tel.: +44 191 222 8101, mobile: +44 777 613 4181.
E-mail address: Ignazio.viola@ncl.ac.uk (I.M. Viola).
URL: http://www.ignazioviola.com (I.M. Viola).

[1] Formerly.
[2] Since September 2010.

0894-1777/$ - see front matter Crown Copyright © 2011 Published by Elsevier Inc. All rights reserved.
doi:10.1016/j.expthermflusci.2011.06.009

Nomenclature

Angle of attack (AoA) The angle between the sail chord and the apparent wind direction.
Apparent and true wind The '*apparent wind*' is the wind experienced by a sailing yacht and results from the vector difference between the atmospheric boundary layer, namely the '*true wind*', and the yacht velocity (Fig. 1). The change in direction of the apparent wind velocity with the height is called the '*twist*'.
Apparent wind angle (AWA) The supplementary angle between the yacht velocity and the apparent wind velocity.
Drive force Aerodynamic force component in the direction of the yacht velocity.
Headsail and mainsail Sail set forward and behind the mast, respectively, in a yacht with a single mast.
Slot effect The effect of the gap between the sails on their performance.
Upwash and downwash Deflection of the streamlines beyond the top of a sail, and behind a sail, respectively, due to the generation of lift. Also used to describe the deflection of streamlines upstream and downstream of a sail, respectively, due to the generation of lift.
Upwind and downwind Directions of the yacht with respect to the true wind. A yacht sails upwind and downwind when the angle between her velocity and the true wind is lower and higher than 90° respectively.
Windward and leeward Side of the sail facing the wind and hidden from the wind, respectively.

flutes. Pressures were carried along the sail in the core-flutes to the sail foot. Pressure tubes carried the pressure from the sail foot to the transducers, which were placed in the cockpit. The sails were perforated along 5 horizontal sections. On the 5 mainsail sections, 9, 11, 13 and 14 holes were used on the top to the bottom sections, respectively. On the 4 headsail sections, 7, 8, 11 and 15 holes were used on the top to the bottom sections, respectively. To measure the leeward side of the sail, tape was used to close the holes on the windward side, and vice versa. In order to correctly model the leading edge flow field, the sails were chamfered at about 20° on the windward side to produce a sharp leading edge. Additional details of the sail construction can be found in Fluck et al. [3].

The sails were fixed onto a model-scale yacht with a rigid mast, and were tested in the YRU Wind Tunnel (Fig. 2). The wind tunnel is an open jet with a test section 7 m wide and 3.5 m high.

Four different mainsail and headsail trims, four AWAs (16°, 20°, 24° and 28°), several heel angles (from 0° to 20°), and several twists of the onset flow were tested. The results presented and discussed in the paper are restricted to those measured in upright sailing conditions and with no twist in the onset flow.

The reference static pressure p_∞ was provided by the static tap of a Pitot-static tube, which was located approximately at the same height as the top of the mast and 6 h upstream of the model (where h = 2.3 m is the model height). The difference between the total pressure tap and the static tap of the same Pitot-static tube was used to measure the reference dynamic pressure q_∞ = 32.5 Pa.

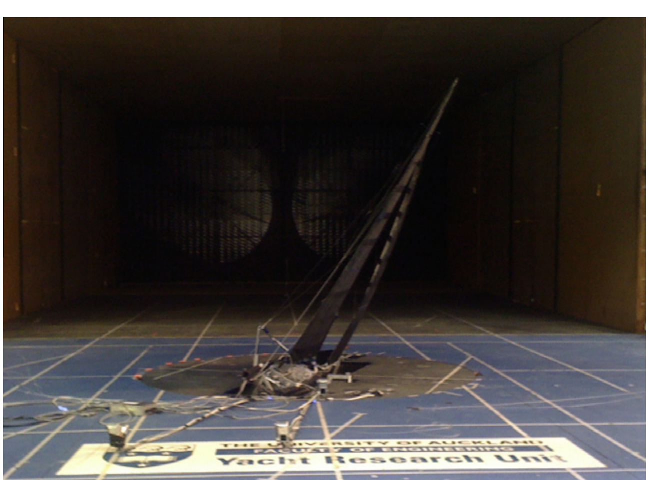

Fig. 1. Wind velocity triangle for a yacht sailing upwind.

The Reynolds number Re based on the average chord length c = 0.49 m was Re = 2.3 × 10^5. The pressure measurement accuracy was estimated to be about ±0.5 Pa.

The same pressure system was used to measure the pressure distributions on full-scale sails. Pressures from 30 to 33 pressure taps on the mainsail and headsail, respectively, of a Sparkman & Stephens 24-foot yacht (SS24) were measured. Several sail trims and apparent wind angles were tested. The reference static pressure p_∞ was measured inside the yacht cabin. The dynamic pressure q_∞ was measured with Pitot-static tubes fixed onto a pole attached to the stern of the yacht. More details can be found in [9]. Subsequent analysis showed that the dynamic pressure measured at this location was about 20% higher than the estimated far-field dynamic pressure due to the influence of the yacht and sails on the pressure measuring system. In the present paper, the corrected dynamic pressure has been used. The full-scale Re based on the mean chord (1.5 m) and the mean apparent wind velocity (6 m/s) was Re = 6.1 × 10^5. Fig. 3 shows a schematic drawing of the AC33 and the SS24 sailplans.

Both in the wind-tunnel tests and in the full-scale test, the pressure distributions showed the same qualitative trends with the AWA and the trim variations. The measured pressure trends can be explained in terms of conventional thin airfoil theory and the aerodynamic properties of separation bubbles. In the following, the measured pressure distributions on the sail sections are related to the angle of attack (AoA), which resulted from the sail trims and the AWAs (see Fig. 1).

3. Pressure distributions on the headsail

3.1. Ideal AoA

The maximum drive force was achieved when the headsail was trimmed at, or slightly higher than, the '*ideal*' AoA, i.e. when the local flow is tangent to the sail at the leading edge (LE). The stagnation point is then located at the LE, where the pressure coefficient, defined as $Cp = (p - p_\infty)/q_\infty$, is $Cp = 1$.

Fig. 4 shows schematic diagrams of the anticipated streamlines around horizontal headsail sections trimmed at different AoAs. *Cps* plotted against the corresponding non-dimensional chords x/c are also shown. In particular, Fig. 4B shows the streamlines around the headsail section trimmed at the ideal AoA.

On cambered sails, at the ideal AoA, an attached boundary layer grows from the LE on both sides of the sail. The sail curvature leads to suction and pressure peaks on the leeward and windward sides respectively, related to the position of maximum camber. At the trailing edge (TE), Cp is about zero or is slightly negative.